SCIENTIFIC REPORTS

OPEN

SUBJECT AREAS:
PROTEIN PURIFICATION
EXPRESSION SYSTEMS
KINASES
CHROMATOGRAPHY

Received
18 February 2013

Accepted
19 March 2013

Published
5 April 2013

Correspondence and requests for materials should be addressed to D.M.R. (draben@jhmi.edu)

Bacterial expression strategies for several *Sus scrofa* diacylglycerol kinase alpha constructs: solubility challenges

Elizabeth J. Petro & Daniel M. Raben

Department of Biological Chemistry, The Johns Hopkins University School of Medicine, Baltimore, MD.

We pursued several strategies for expressing either full-length *Sus scrofa* diacylglycerol kinase (DGK) alpha or the catalytic domain (alphacat) in *Escherichia coli*. Alphacat could be extracted, refolded, and purified from inclusion bodies, but when subjected to analytical gel filtration chromatography, it elutes in the void volume, in what we conclude are microscopic aggregates unsuitable for x-ray crystallography. Adding glutathione S-transferase, thioredoxin, or maltose binding protein as N-terminal fusion tags did not improve alphacat's solubility. Coexpressing with bacterial chaperones increased the yield of alphacat in the supernatant after high-speed centrifugation, but the protein still elutes in the void upon analytical gel filtration chromatography. We believe our work will be of interest to those interested in the structure of eukaryotic DGKs, so that they know which expression strategies have already been tried, as well as to those interested in protein folding and those interested in chaperone/target-protein interactions.

Diacylglycerol kinases (DGKs) are a family of enzymes in eukaryotes that catalyze the transfer of the γ-phosphoryl from adenosine triphosphate (ATP) onto the hydroxyl of diacylglycerol to produce adenosine diphosphate (ADP) and phosphatidic acid. Most mammalian DGKs are interfacial enzymes, catalyzing reactions at the two-dimensional interface between the membrane and the aqueous phase.

Eukaryotic DGKs have been implicated in a number of physiological roles and human diseases[1,2]. Understanding the structure of these enzymes would bring insight into their activity, open doors to DGK modulator production and impact not only lipid signaling research but also medicine. Furthermore, little is known about the function of lipid kinases. Unlike their relatives with soluble substrates, the interfacial properties of these kinases greatly increase the technical difficulty for research. Lessons learned from DGKs might be applied to other lipid kinases, or indeed other interfacial enzymes. Most research to date revolves around protein-protein interactions, whereas much less concentrates on activity between lipids and proteins. Purification techniques and structural studies between DGKs interactions with DAG may be applied to other proteins that interact with lipids. Applications for this research are endless: not only could *de novo* protein lipid interactions be developed, but also improvements to drug delivery systems would further advance medicine into a new era.

Most work on eukaryotic DGKs has been conducted on those isolated from endogenous sources. Eukaryotic DGKs have been partially purified from rat liver[3], rat brain[4–6], bovine brain[7], bovine thymus[8], human platelets[9], porcine brain[5], porcine testis[10,11], porcine submaxillary glands[12,13], baboon brain[14], 3T3 mouse fibroblast cells[5,12,13,15–18], *Drosophila* heads[19], and *Caltharanthus roseus* suspension-cultured cells[20], and they have been purified to apparent homogeneity from porcine brain[21–23], porcine thymus[12,13,16,24–26], bovine brain[27], bovine testis[12,13,15,16], rat brain[28–30], human platelets[9], human white blood cells[31], and *Microsporum gypseum* suspension-cultured cells[32]. While purified DGKs from endogenous sources have been invaluable for studying their enzymology, these sources are not amenable to producing enough protein for pursuing structural studies.

Recombinant forms of eukaryotic DGKs have been expressed in *E. coli*[33,34], in COS-7 cells[33,35,36], in COS-1 monkey kidney cells[12,13], in Jurkat human T cells[35,37], in HEK293 human embryonic kidney cells[35,38], and in Sf21 *Spodoptera frugiperda* cells[39,40] and have been partially purified from HEK293 cells[41], COS-7 cells[42], *Dictyostelium discoideum*[43,44], *E. coli*[41,45–49], and Sf21 cells[50]. In only two cases to our knowledge has a eukaryotic DGK been purified to apparent homogeneity from a recombinant source: porcine DGK alpha was purified to apparent homogeneity after being expressed in the *Saccharomyces cerevisiae* strain WY294[12], and human DGK theta was purified to apparent homogeneity after being expressed in HEK293 cells[51]. Truncations of the accessory (not catalytic) domains of eukaryotic DGKs have been expressed recombinantly with more success[13,36,52].

As such, little is known about the structure of DGKs, particularly of the catalytic domain. The catalytic domain is so-called because it is a region of primary sequence homology that makes up the gene family. Furthermore, this domain from *S. scrofa* DGK alpha, when expressed in COS-7 cells, was reported to be catalytically competent[42], possessing similar enzymatic properties to the full-length enzyme, demonstrating that all of the determinants for the catalytic reaction, including binding sites for the two substrates, are located in this region of the protein. But whereas a nuclear magnetic resonance (NMR) structure of the N-terminus of *Homo sapiens* DGK alpha has been reported[53], as have an NMR structure of the second C1 domain[54] and an x-ray crystal structure of the SAM domain from *H. sapiens* DGK delta[55], no structures of any part of the catalytic domain from any eukaryotic DGK have yet been published.

We therefore set out to express the catalytic domain of a eukaryotic DGK. Our approach was to express either full-length or just the catalytic domain of *S. scrofa* DGK-alpha (the best-studied of the eukaryotic DGKs) in *E. coli* with the purpose of producing large amounts of soluble protein for structural studies.

Results

pT71myc. *Cloning, expression, refolding, purification, and analytical gel filtration of alphacat in pT71myc*. The alphacat construct consists of residues 333–733 of *S. scrofa* DGK alpha, and is so named because it includes the catalytic domain, which is annotated on the Conserved Domain Database[56] as LCB5. The missing N-terminal residues include the EF-hand motifs and C1 domains; alphacat lacks the C-terminal cysteine (Figure 1a). This construct was cloned into pT71myc, which adds to the N-terminus of the protein a fusion tag consisting of hexahistidine, a thrombin proteolytic site, a myc tag, and a Tobacco Etch Virus (TEV) protease site. The total mass of this protein construct (including the fusion tag) predicted to be 49.8 kD, and the isoelectric point (pI) is 6.99.

Expression of alphacat in the Rosetta™(DE3) (Novagen®) strain of *E. coli* was induced by adding isopropyl-β-D-thiogalactopyranoside (IPTG). When compared to uninduced control, the induced lysate expressed an additional band, easily detectable by Coomassie staining, that migrates between the 40 kD and 50 kD molecular weight standards during sodium dodecyl sulfate polyacrylamide gel electrophoresis (SDS-PAGE), consistent with the predicted size of the fusion protein of 49.8 kD. This band was also recognized by an anti(α)-histidine antibody on immunoblots (Figure 1b), consistent with its expressing the epitope tag.

The alphacat in pT71myc construct, however, produced mostly insoluble protein: when the bacterial lysate was centrifuged, most of the protein remained in the pellet and was not observed in the supernatant (Figure 1c). When washed with 2 M urea and 2% (v/v) Triton X-100, the vast majority of alphacat remained in the pellet rather than the supernatant, leading us to conclude that the expressed protein went into inclusion bodies[57]. Alphacat could be extracted from inclusion bodies using 6.8 M guanidinium chloride, and refolded by snap-diluting fiftyfold into ice-cold buffer (Figure 1d). This refolded alphacat could then be recovered from the supernatant after high-speed centrifugation. This supernatant could be purified by nickel-nitriloacetic acid (Ni-NTA) chromatography (Figure 1d).

Because monodispersity is considered a valuable quality of proteins expressed for structural studies, the affinity-purified fraction was subjected to analytical gel filtration. If the protein is monodisperse, it will elute as a single peak at the appropriate molecular weight: for alphacat in pT71myc, this would be at 49.8 kD (between the 29 kD carbonic anhydrase and the 66 kD albumin molecular weight standards) if it is a monomer, at 99.6 kD (between albumin and the 150 kD alcohol dehydrogenase) if it is a dimer, etc. Although refolded purified alphacat was recovered from the supernatant after centrifugation, when subjected to Sephadex® G-200 gel filtration chromatography, the protein eluted in the void volume (Figure 1e).

Cloning, expression, purification, and analytical gel filtration of alphacat in pT71myc coexpressed with bacterial chaperones. Coexpression with bacterial chaperones is a commonly used strategy to improve the yield and solubility of recombinantly expressed proteins in *E. coli*[58–60]. In an attempt to improve the solubility of alphacat, we therefore coexpressed it with each of five sets of bacterial chaperones: GroEL/ES, Trigger Factor (TF), GroEL/ES/TF, DnaK/DnaJ/GrpE, and DnaK/DnaJ/GrpE/ClpB. The molecular weights of the bacterial chaperones are as follows: GroEL = 57.4 kD; GroES = 10.4 kD; TF = 48.2 kD; DnaK = 69.1 kD; DnaJ = 41.1 kD; GrpE = 21.8 kD; ClpB = 95.9 kD.

The Rosetta™(DE3) strain of *E. coli*, which had been used to express the alphacat in pT71myc above, contains pRARE, a plasmid encoding the tRNAs for codons that are commonly used by eukaryotes but rarely used by *E. coli*. pRARE, however, contains the same antibiotic resistance gene as the plasmid encoding the chaperones, therefore to be able to select for expression of the chaperones, we switched to the BL21(DE3) strain of *E. coli*. Alphacat coexpressed with GroEL, GroES, TF, and DnaK robustly expressed when induced with IPTG, as detected by Coomassie staining after SDS-PAGE (Figure 2a). DnaJ, GrpE, and ClpB expression were not detectable by Coomassie staining.

To identify which chaperone constructs enhanced solubility of alphacat, they were coexpressed either at 37°C for three hours, or at 16°C overnight. Coexpression of either GroEL/ES or GroEL/ES/TF at 16°C overnight, and to a lesser extent, coexpression of GroEL/ES/TF at 37°C for three hours, resulted in an increase in alphacat detected in the supernatant following centrifugation of the lysate (Figure 2a).

As can be seen in Figure 2a, in addition to the alphacat band, the α-DGK-alpha antibody recognizes higher-molecular weight bands (in addition to the alphacat band) in the GroEL-containing lanes of the immunoblots. Because the α-DGK-alpha antibody recognizes GroEL (Figure 2b), we concluded that the 60 kD bands in the immunoblot in Figure 2a are GroEL.

Alphacat coexpressed with GroEL/ES at 16°C overnight was partially purified by Ni-NTA chromatography, and GroEL (the upper band) coeluted with alphacat (the lower band) from the Ni-NTA resin (Figure 2c). When the Ni-NTA eluate was subjected to Sephadex® G-200 size-exclusion chromatography, alphacat and GroEL coeluted in the void volume (Figure 2d).

If the GroEL/ES complex had never released alphacat, it would be predicted to form a complex made of fourteen GroEL monomers and seven GroES monomers, plus the alphacat, at least 920 kD in size, indeed larger than the ~200-kD void volume of the Sephadex® G-200 resin. 1 mM ATP has been reported to be sufficient to cause GroEL to release its substrates[61]. To test whether 1 mM ATP would cause GroEL to release alphacat, we lysed and purified alphacat from the co-expressing lysates in the presence of 1 mM ATP. 1 mM ATP has no effect on the Ni-NTA purification of alphacat and GroEL/ES, and GroEL continued to coelute with alphacat from the Ni-NTA resin (Figure 2e).

Cloning and expression of full-length DGK alpha in pT71myc. The cDNA for full-length *S. scrofa* DGK alpha (amino acids 1-734) was cloned into the pT71myc vector, adding the same N-terminal fusion tag as described above for the alphacat construct, consisting of a hexahistidine, a thrombin proteolytic site, a myc tag, and a TEV protease site (Figure 3a). The total mass of this protein construct (including the fusion tag) and the pI are predicted to be 87.5 kD and 6.10 respectively.

When full-length DGK alpha in pT71myc is transformed into the BL21(DE3) strain of *E. coli*, it expresses readily after induction with IPTG, producing a band, easily detectable by Coomassie staining after SDS-PAGE, that migrates between the 70 kD and 100 kD molecular weight markers, consistent with the predicted size of 87.5 kD, and is recognized by an α-histidine antibody on immunoblots

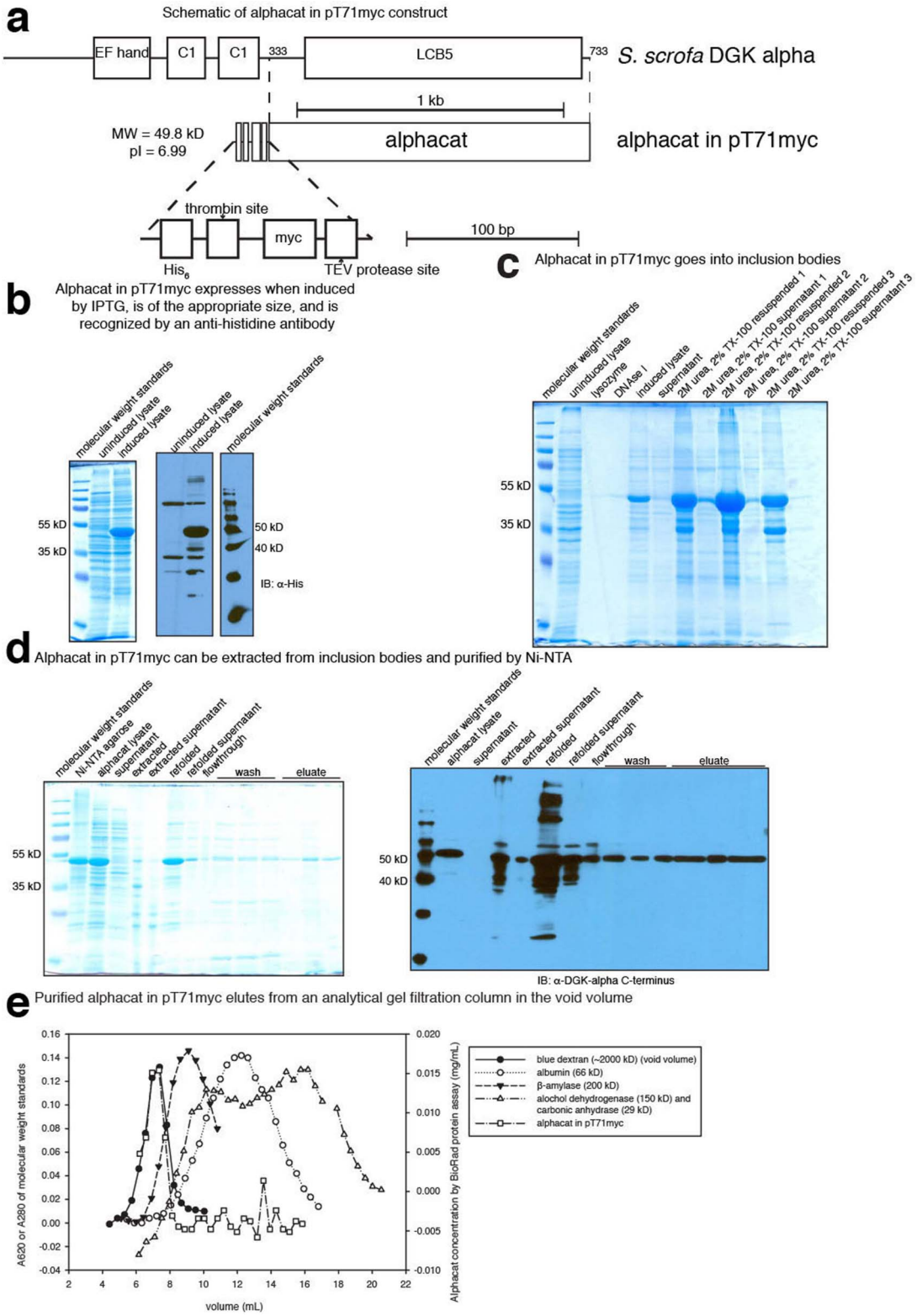

Figure 1 | Cloning, expression, refolding, purification, and analytical gel filtration of alphacat in pT71myc. (a) Top, a schematic of *S. scrofa* DGK alpha. Middle, a schematic of "alphacat", which consists of residues 333–733 of DGK alpha, including the LCB5 domain, but missing the C-terminal cysteine. Bottom, a magnification of the epitope tag region of alphacat in pT71myc. pT71myc adds to the N-terminus of the protein a fusion tag consisting of a hexahistidine, a thrombin proteolytic site, a myc tag, and a TEV protease site. The total mass of this protein construct (including the fusion tag) and pI are predicted to be 49.8 kD and 6.99, respectively. (b) SDS-PAGE of 12% acrylamide gels followed by: left, Coomassie staining; right, immunoblot against histidine. IB, immunoblot. (c) SDS-PAGE of a 12% acrylamide gel followed by Coomassie staining. DNAse I was added to the lysate to 10 U per mL. TX-100, Triton X-100. (d) SDS-PAGE of 12% acrylamide gels followed by: top, Coomassie staining; bottom, immunoblot against DGK alpha C-terminus. (e) Elution volumes of molecular weight standards and of purified alphacat from a Sephadex® G-200 column. Left vertical axis, the absorbance at 620 nm (A620) of blue dextran elution and the absorbance at 280 nm (A280) of protein standard elutions. Right vertical axis, protein concentration of eluted alphacat, as measured by the Bio-Rad Protein Assay.

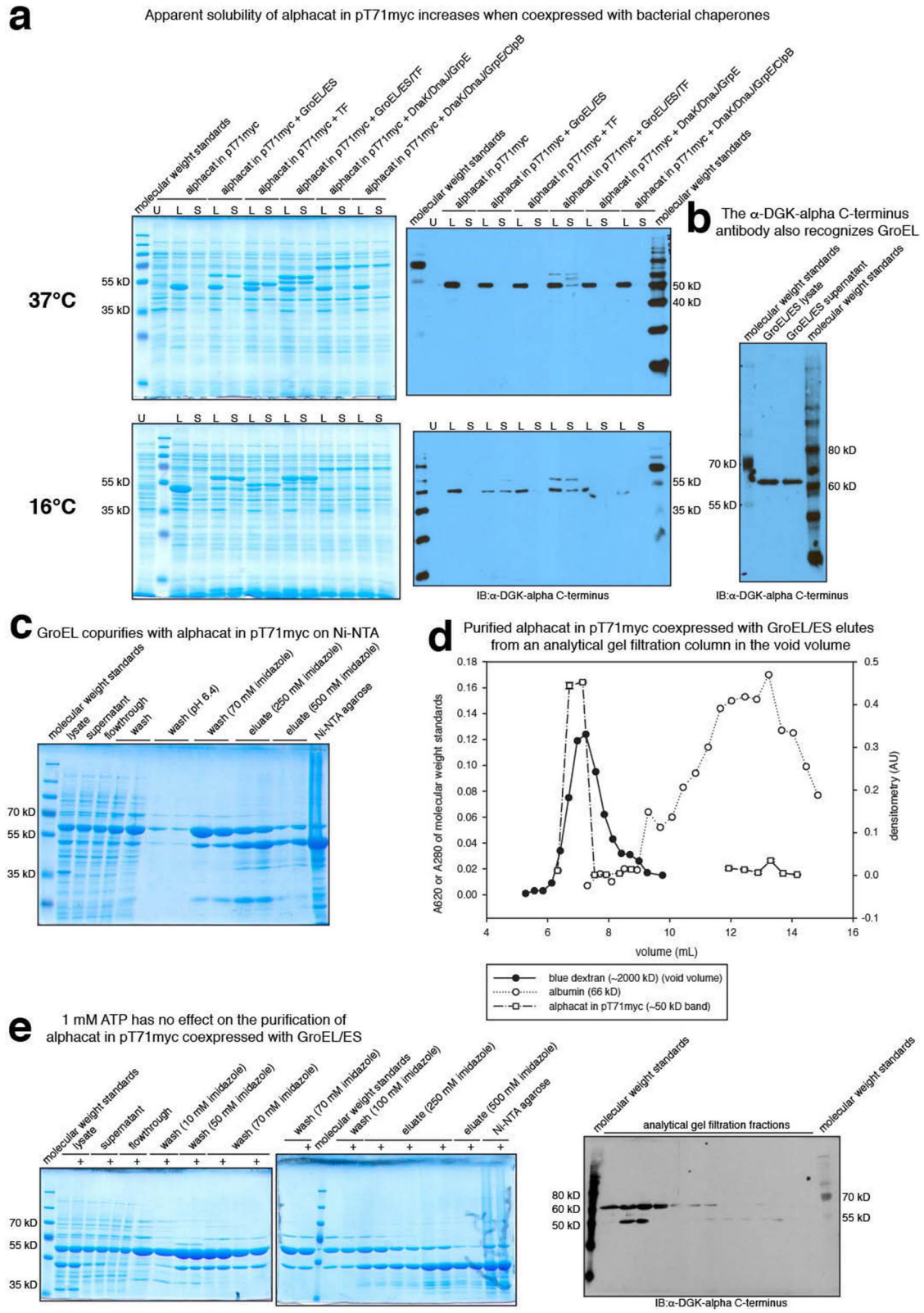

Figure 2 | Expression, purification, and analytical gel filtration of alphacat in pT71myc coexpressed with bacterial chaperones. (a) SDS-PAGE of 12% acrylamide gels followed by: left, Coomassie staining; right, immunoblot against DGK alpha C-terminus; top, induced at 37°C for three hours; bottom, induced at 16°C overnight. U, uninduced; L, lysate; S, supernatant (after removing insoluble from lysate). (b) SDS-PAGE of an 8% acrylamide gel followed by immunoblotting against DGK alpha C-terminus. (c) SDS-PAGE of a 10% acrylamide gel followed by Coomassie staining. (d) Top, elution volumes of molecular weight standards and of purified alphacat from a Sephadex® G-200 column. Left vertical axis, A620 of blue dextran elution and A280 of protein standard elutions. Right vertical axis, quantification of the immunoblot signal from the blot shown at bottom, mean ± standard deviation (SD) (arbitrary units (AU)). Densitometry of the ~50 kD band was measured three times from the same film using ImageJ. Bottom, SDS-PAGE of a 10% acrylamide gel followed by immunoblotting against DGK alpha C-terminus. (e) SDS-PAGE of a 10% acrylamide gel followed by Coomassie staining. The lanes marked "+" were purified in the presence of 1 mM ATP.

(Figure 3b), consistent with its expressing the epitope tag, as expected. This construct, however, like alphacat in pT71myc, also produces insoluble protein: when the bacterial lysate is centrifuged, the protein remains in the pellet.

In order to determine whether any of the sets of chaperones could improve this construct's solubility, DGK alpha in pT71myc and each of the sets of chaperones were coexpressed either at 37°C for three hours, or at 16°C overnight. At 16°C, co-expression of each of the sets of plasmids increased the amount DGK alpha detected in the supernatant after centrifugation (Figure 3b). The set that increased the amount to the greatest extent was GroEL/ES/TF, but even in this case, most of the protein remains in the pellet (Figure 3b).

Cloning, expression, purification and analytical gel filtration of alphacat in pGEX-4T2 coexpressed with bacterial chaperones. Translational folding partners have been reported to improve the solubility of proteins expressed in *E. coli*[62–65]. In addition to being a useful epitope tag for affinity purification[66], glutathione-S-transferase (GST) is one such fusion tag that has been reported to improve the solubility of target proteins to which it has been fused[67]. In fact, GST fusion tags have been successfully used to express the EF-hands of DGK alpha and gamma (although not beta) in *E. coli*[52]. In an attempt to improve the solubility of recombinantly expressed alphacat, we therefore cloned alphacat into the pGEX-4T2 vector (Figure 4a). This vector introduces GST from *Schistosoma japonicum* followed by a

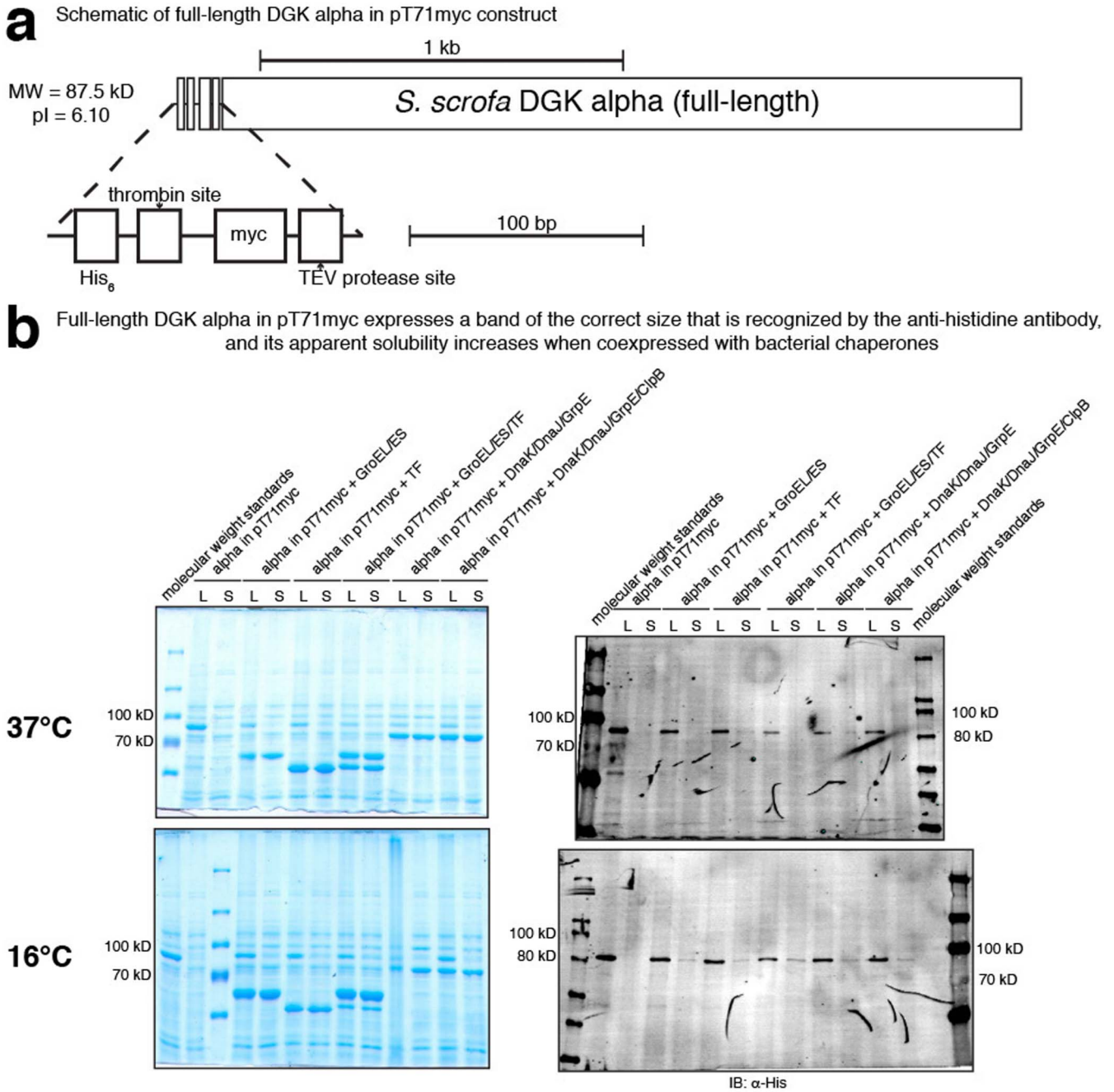

Figure 3 | Cloning and expression of full-length DGK alpha in pT71myc. (a) Top, schematic of full-length *S. scrofa* DGK alpha in pT71myc. Bottom, a magnification of the epitope tag region of alpha in pT71myc. pT71myc adds to the N-terminus of the protein a fusion tag consisting of a hexahistidine, a thrombin proteolytic site, a myc tag, and a TEV protease site. The total mass of this protein construct (including the fusion tag) and pI are predicted to be 87.5 kD and 6.10, respectively. The epitope-tagged region of the construct is magnified for clarity. (b) SDS-PAGE of 8% acrylamide gels followed by: left, Coomassie staining; right, immunoblotting against hexahistidine; top, induced at 37°C for three hours; bottom, induced at 16°C overnight. L, lysate; S, supernatant (after removing insoluble from lysate).

thrombin proteolytic site at the N-terminus of the protein. The total mass of this protein construct (including the fusion tag) and pI are predicted to be 71.6 kD and 6.97, respectively. DNA sequencing confirmed the proper leader sequence, including the entire GST gene and the thrombin proteolytic site, and the insertion of alphacat.

When alphacat in pGEX-4T2 was transformed into BL21 (DE3) strain of *E. coli*, it expressed readily after induction with IPTG, producing a band, easily detectable by Coomassie staining after SDS-PAGE, that runs between the 60 kD and 70 kD molecular weight markers, slightly faster than its predicted size of 71.6 kD, and was recognized by an α-DGK-alpha antibody by immunoblot

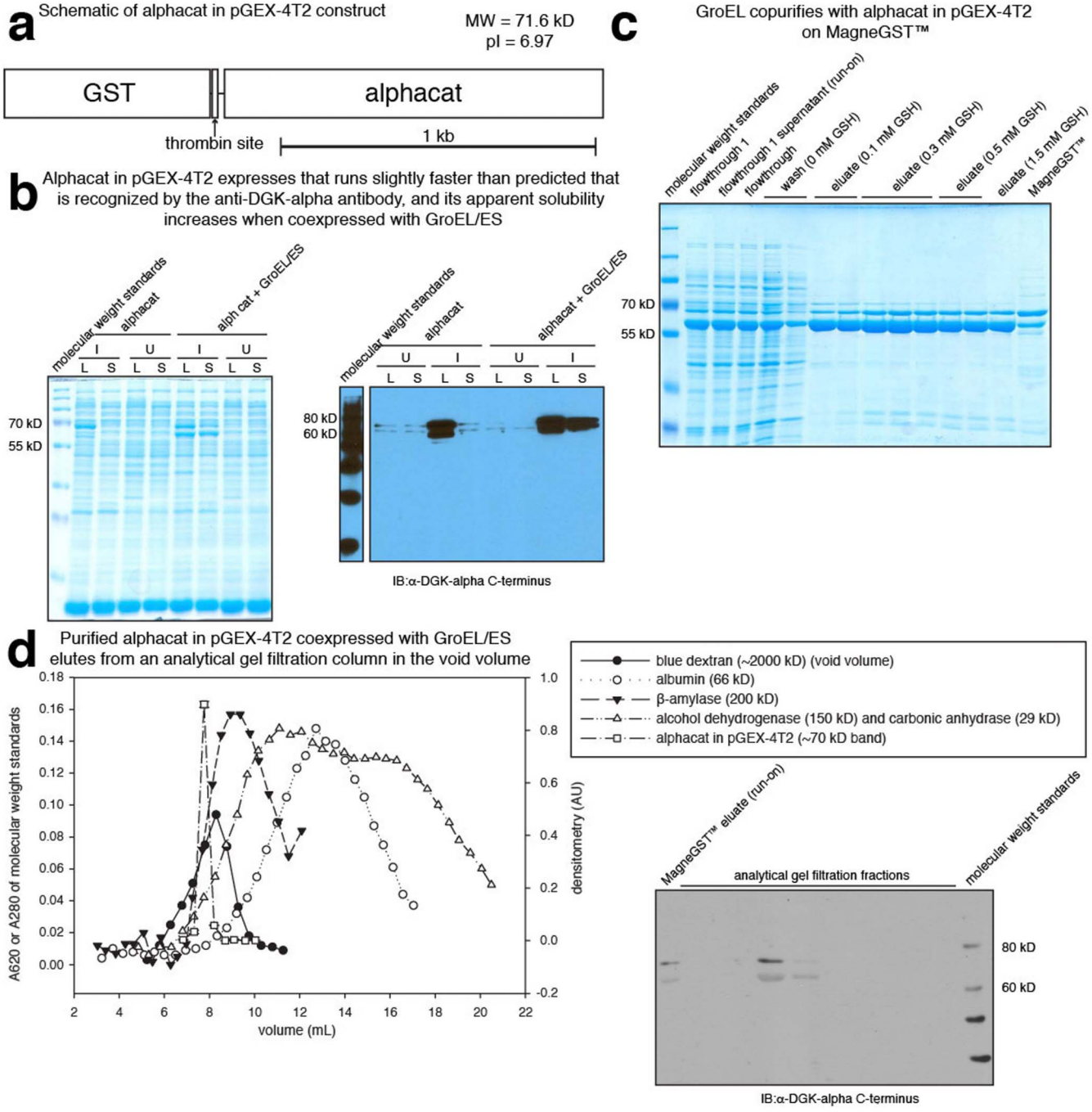

Figure 4 | Cloning, expression, purification, and analytical gel filtration of alphacat in pGEX-4T2 coexpressed with bacterial chaperones. (a) "Alphacat" consists of residues 333–733 of *S. scrofa* DGK alpha. pGEX-4T2 adds to the N-terminus of the protein a fusion tag consisting of *S. japonicum* GST followed by a thrombin proteolytic site. The total mass of this protein construct (including the fusion tag) and pI are predicted to be 71.6 kD and 6.97, respectively. (b) SDS-PAGE of 12% acrylamide gels followed by: left, Coomassie staining; right, immunoblotting against against DGK alpha C-terminus. I, induced; U, uninduced; L, lysate; S, supernatant (after removing insoluble from lysate). (c) SDS-PAGE of a 10% acrylamide gel followed by Coomassie staining. This sample was purified after having previously flowed through MagneGST™. The insoluble fraction was removed before loading onto fresh MagneGST™. GSH, glutathione. (d) Elution volumes of molecular weight standards and of purified alphacat from a Sephadex® G-200 column. Left vertical axis, A620 of blue dextran elution and A280 of protein standard elutions. Right vertical axis, quantification of the immunoblot signal from the blot shown at right, mean ± SD (AU). Densitometry of the ~70 kD band was measured three times from the same film using ImageJ. Right, SDS-PAGE of an 8% acrylamide gel followed by immunoblotting against DGK alpha C-terminus.

(Figure 4b). As we observed with alphacat in pT71myc, the alphacat in pGEX-4T2 construct produced insoluble protein, as measured by detection either by Coomassie staining or immunoblot following SDS-PAGE following whole lysate centrifugation. As we also observed with alphacat in pT71myc, coexpressing GroEL/ES increased the amount of GST-tagged alphacat detected (either by Coomassie or immunoblot) in the supernatant after centrifugation. (As above, GroEL is recognized by the α-DGK-alpha antibody; in this case, GroEL is the lower band, and alphacat is the upper band.)

Alphacat in pGEX-4T2 coexpressed with GroEL/ES could be partially purified by affinity chromatography, but, once again, as with alphacat in pT71myc, GroEL coeluted with alphacat from the glutathione particles (Figure 4c). When the eluate was subjected to Sephadex® G-200 analytical gel filtration chromatography, the two proteins coeluted in the void volume (Figure 4d).

Cloning and expression of alphacat and full-length DGK alpha in pET32a coexpressed with bacterial chaperones. In another attempt to improve the solubility of alphacat and full-length DGK alpha, these proteins were each cloned into the plasmid pET32a, which adds to the N-terminus of the protein a fusion tag consisting of *E. coli* thioredoxin (TRX), which has been reported to improve the solubility of target proteins[62,68]. This plasmid also adds to the N-terminus hexahistidine, which can be used for affinity purification (Figure 5a). We also added either a TEV protease site or a PreScission Protease site, which could be used to proteolytically remove the fusion tag, and named the constructs accordingly (alphacat TEV in pET32a, alphacat PP in pET32a, and full-length alpha TEV in pET32a). While cloning, we also took the opportunity to add back the 734th residue, a cysteine, to the C-terminus of alphacat, and to remove the initial methionine from full-length DGK alpha. The total mass of the alphacat construct (including the fusion tag, and with either protease site) is predicted to be 64.4 kD, and the pI is predicted to be 6.19. The total mass and pI of the full-length DGK alpha construct are predicted to be 102.0 kD and 5.84, respectively.

When these pET32a constructs were transformed into the BL21(DE3) strain of *E. coli*, they each expressed readily after induction with IPTG, producing a band that runs at the predicted size, which was easily detectable by Coomassie staining after SDS-PAGE (Figure 5b, top left). As we observed with our other constructs, the TRX-tagged alphacat and full-length DGK alpha constructs produced insoluble protein, as measured by detection by Coomassie staining after SDS-PAGE in the supernatant after centrifugation. To determine whether coexpression with bacterial chaperones improves the solubility of these constructs, we coexpressed each of the three pET32a constructs with GroEL/ES, as well as alphacat TEV with each of the five sets of chaperones. Unlike alphacat in pT71myc or alphacat in pGEX-4T2, coexpressing with chaperones did not improve the solubility of either alphacat or full-length DGK alpha in pET32a, as measured by Coomassie staining or immunoblotting following SDS-PAGE following centrifugation (Figure 5b, right). Once again, GroEL is recognized by the α-DGK-alpha antibody; in this case, GroEL is the lower band, and alphacat is the upper band. GroEL is soluble after centrifugation, whereas alphacat TEV in pET32a is not.

Cloning, expression, purification, and analytical gel filtration of alphacat and full-length DGK alpha in pET28-HisMBP-FLAGpp. Maltose binding protein (MBP) has been reported to improve the solubility of target proteins to which it has been fused[63,69,70]. We cloned both alphacat and full-length DGK alpha into the pET28-HisMBP-FLAGpp plasmid, which adds to the N-terminus of the protein a fusion tag that includes hexahistidine, *Pyrococcus furiosus* MBP, a FLAG tag, and a PreScission Protease site (Figure 6a). As with pET32a, we took the opportunity while cloning to add back the 734th residue, a cysteine, to the C-terminus of alphacat, and to remove the initial methionine from full-length DGK alpha. The total mass and pI of the alphacat and full-length DGK alpha constructs are predicted to be 92.8 kD, 5.51, 130.6 kD, and 5.45, respectively.

When MBP-tagged alphacat or full-length DGK alpha was transformed into the BL21(DE3) strain of *E. coli*, they each expressed readily after induction with IPTG, producing a band, easily detectable by Coomassie staining following SDS-PAGE, of the predicted size that is recognized by the α-DGK-alpha antibody (Figure 6b). The MBP tag does not appear to improve DGK alpha's solubility: the fusion-tagged protein, either alphacat or full-length DGK alpha, while easily detectable in the lysate, remains undetectable in the supernatant by immunoblotting after centrifugation.

For our pT71myc construct, we had observed that although most of the expressed alphacat was in the pellet, the very small amount in the supernatant, even of low enough levels to be undetectable by immunoblotting, could be enriched by affinity purification on Ni-NTA (unpublished observations, EP). We therefore attempted to likewise purify the supernatant of MBP-tagged alphacat by Ni-NTA affinity chromatography to see whether enough alphacat could be enriched to subject to analytical gel filtration chromatography. MBP-tagged alphacat could indeed be enriched by Ni-NTA chromatography (Figure 6c). When the eluate was subjected to Sephadex® G-200 analytical gel filtration chromatography, however, MBP-tagged alphacat eluted in the void volume (Figure 6d), as we had observed with our other constructs.

In another attempt to improve our protein constructs' solubility, after inducing expression in *E. coli* with IPTG we added chloramphenicol to arrest translation, which has been reported in to improve the solubility of other proteins prone to aggregation[71]. Treating the cells with chloramphenicol did not appear to improve the recovery of MBP-tagged alphacat or full-length DGK alpha in the supernatant following centrifugation, as measured by either Coomassie staining or immunoblotting following SDS-PAGE (Figure 6e).

Discussion

For all of the constructs tested, when either full-length *S. scrofa* DGK alpha or just its catalytic domain is expressed in *E. coli*, the recombinant protein is insoluble. Alphacat can be refolded from inclusion bodies, but while it is detectable in the supernatant after high-speed ultracentrifugation, when this soluble fraction is subjected to analytical gel filtration chromatography, alphacat elutes in the void volume. We therefore conclude that the alphacat is forming aggregates unsuitable for pursuit for structural studies.

An alternative explanation is that the alphacat oligomerizes into a complex large enough to elute in the void volume of the Sephadex® G-200 resin. Oligomerization of LCB5 family proteins is not unprecedented: purified *Salmonella typhimurium* YegS recombinantly expressed in *E. coli* elutes as a dimer from a Superdex G200 resin[72], *E. coli* YegS[73] and *Staphylococcus aureus* DgkB[74] recombinantly expressed in *E. coli* each crystallize as dimers, and *H. sapiens* DGK epsilon recombinantly expressed in COS-7 cells has been reported to dimerize based on its migration in perfluorooctanoic acid (PFO)-PAGE[40]. The smallest of the constructs studied in this report is alphacat in pT71myc, with a molecular weight of 49.8 kD. In order for oligomerized alphacat in pT71myc to be larger than β-amylase (200 kD), in front of which we observe it to elute from the Sephadex® G-200 resin, its oligomerization state would have to be at least that of a pentamer (249 kD). Because the most plausible oligomerization states of alphacat would be either a dimer or else a dimer of dimers, we find the microscopic aggregate hypothesis more convincing.

Solubility challenges with expressing eukaryotic DGKs recombinantly in *E. coli* have been previously reported. In one case *S. scrofa* DGK alpha purified from inclusion bodies had no detectable DGK activity[46] (even though *E. coli* lysate overexpressing the same protein does have DGK activity[33]); in another, AtDGK2 from *Arabidopsis thaliana* required a NusA tag in order to express in *E. coli*[48].

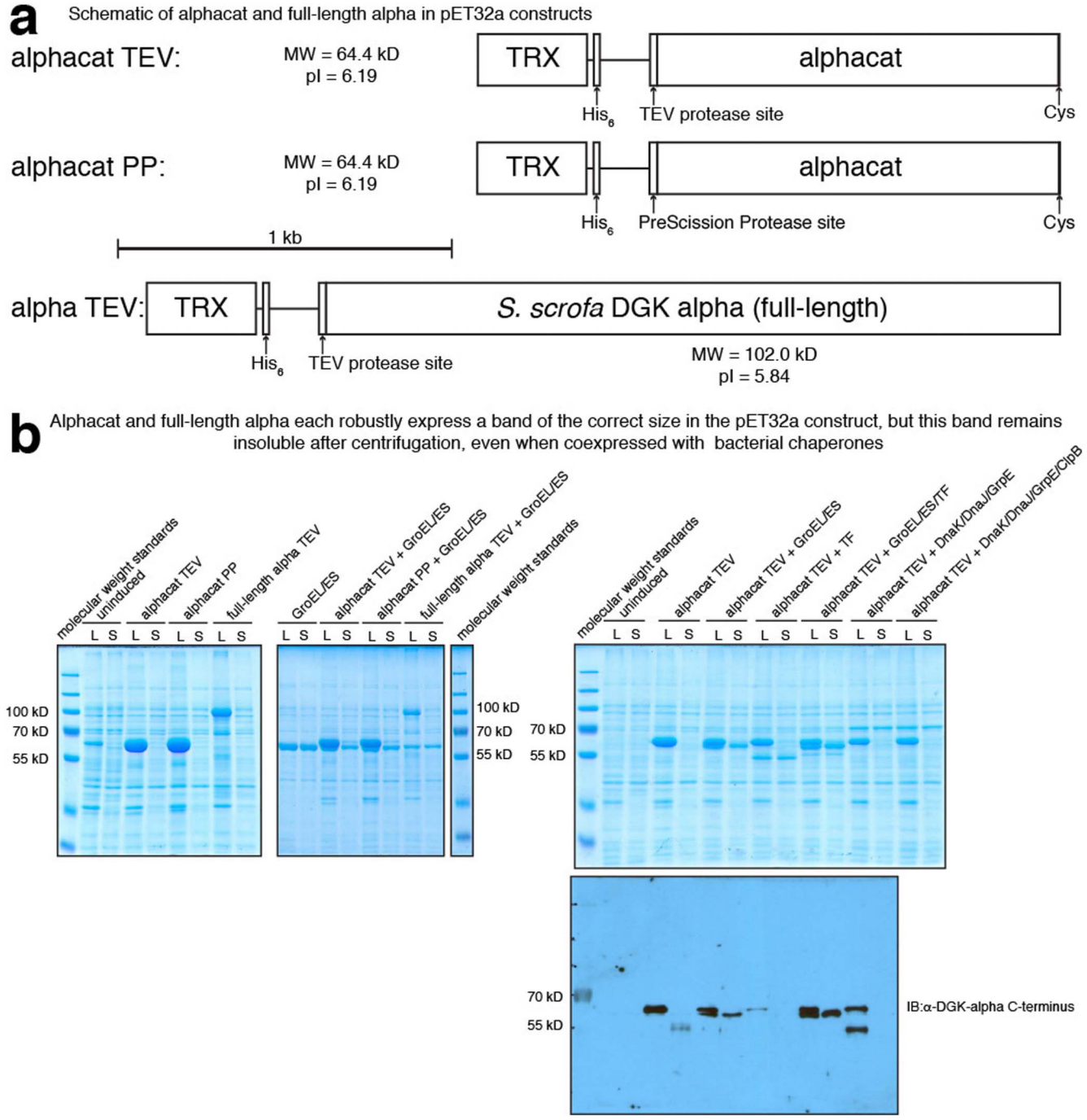

Figure 5 | Cloning and expression of alphacat and full-length DGK alpha in pET32a coexpressed with bacterial chaperones. (a) Top: schematic of alphacat TEV in pET32a construct. ''Alphacat'' consists of residues 333–733 of *S. scrofa* DGK alpha; for this construct, the 734th residue of *S. scrofa* DGK alpha, cysteine, was added back. pET32a adds to the N-terminus of the protein a fusion tag consisting of *E. coli* TRX followed by a hexahistidine tag. For alphacat TEV, a TEV protease site site was added between the fusion tag and alphacat. The total mass of this protein construct (including the fusion tag) and pI are predicted to be 64.4 kD and 6.19, respectively. Middle: schematic of alphacat PP in pET32a construct. Instead of a TEV protease site, a PreScission Protease site was added between the fusion tag and alphacat. The total mass of this protein construct (including the fusion tag) and pI are predicted to be 64.4 kD and 6.19, respectively. Bottom: schematic of full-length *S. scrofa* DGK alpha TEV in pET32a construct. A TEV protease site was added between the fusion tag and DGK alpha, and the initial methionine was removed from DGK alpha. The total mass of this protein construct (including the fusion tag) and pI are predicted to be 102.0 kD and 5.84, respectively. (b) SDS-PAGE of 10% acrylamide gels followed by: top and middle, Coomassie staining; bottom, immunoblot against DGK alpha C-terminus. L, lysate; S, supernatant (after removing insoluble from lysate).

Takahashi *et al.* report that they were unable to express the C-terminal domain of *S. scrofa* DGK alpha in *E. coli* because the cysteine-rich C1 domain rendered it insoluble[36]. Recombinantly expressing LCB5 family proteins in *E. coli* has generally been more successful when those family members are prokaryotic[72–74].

One possible explanation for why recombinant expression of prokaryotic LCB5 family proteins has been more successful than eukaryotic is that prokaryotes have different codon abundances than eukaryotes. Insufficient availability of the appropriate tRNA can lead to ribosome pausing, frameshifts, deletions, mistranslations, aborted

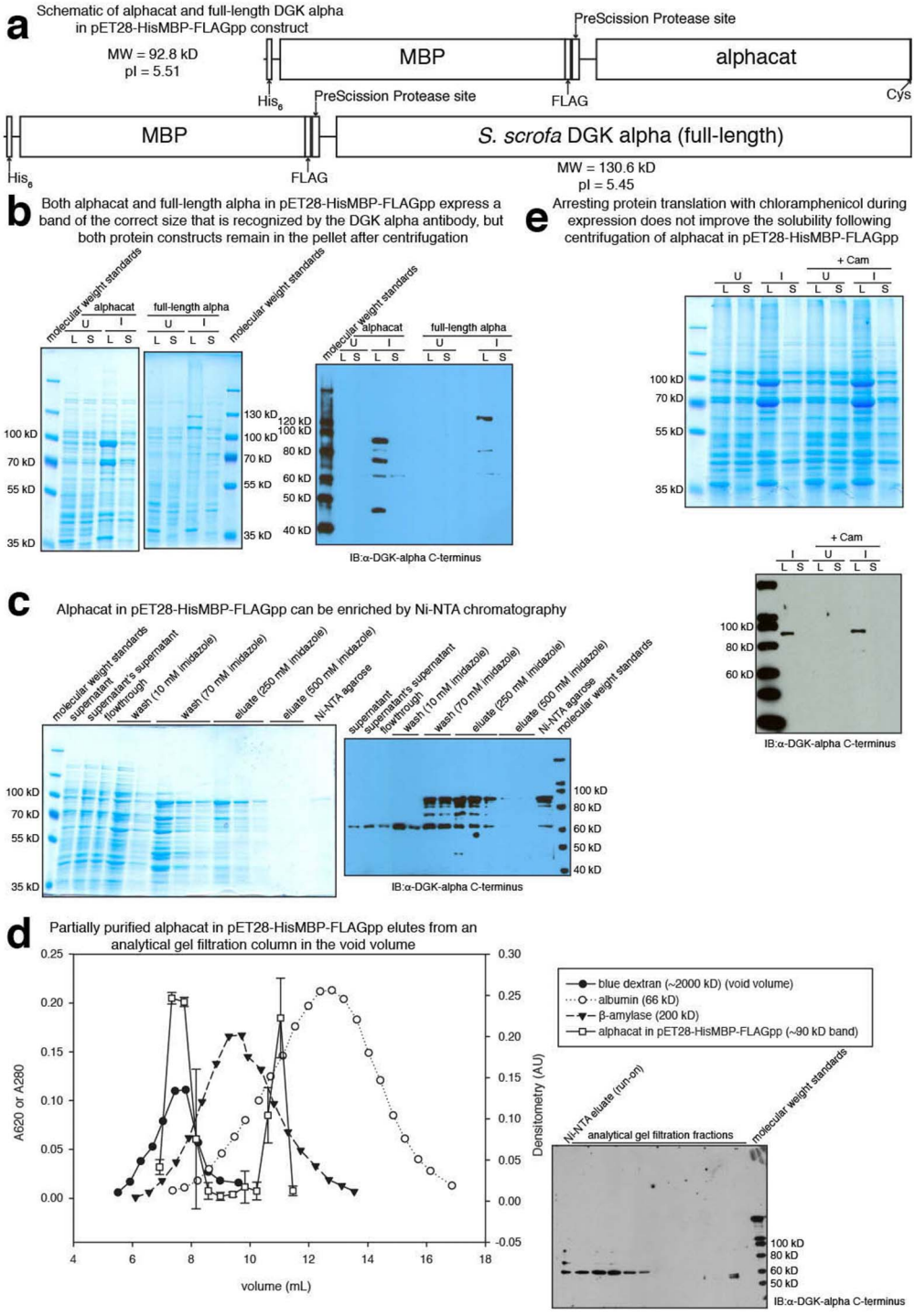

Figure 6 | Cloning, expression, partial purification, and analytical gel filtration of alphacat and full-length DGK alpha in pET28-HisMBP-FLAGpp. (a) Top, schematic of alphacat in HisMBP-FLAGpp construct. ''Alphacat'' consists of residues 333–733 of *S. scrofa* DGK alpha; for this construct, the 734th residue of *S. scrofa* DGK alpha, cysteine, was added back. pET28-HisMBP-FLAGpp adds to the N-terminus of the protein a fusion tag consisting of a hexahistidine tag, followed by *P. furiosus* maltose-binding protein (MBP) fusion tag, followed by a FLAG tag, followed by a PreScission Protease site. The total mass of the protein construct (including the fusion tag) and pI are predicted to be 92.8 kD and 5.51, respectively. Bottom, schematic of full-length *S. scrofa* DGK alpha construct. The total mass of the protein construct (including the fusion tag) and pI are predicted to be 130.6 kD and 5.45, respectively. (b) SDS-PAGE of 8% acrylamide gels followed by: top, Coomassie staining; bottom, immunoblotting against DGK alpha C-terminus. U, ininduced; I, induced; L, lysate; S, supernatant (after removing insoluble from lysate). (c) SDS-PAGE followed by: left, Coomassie staining; right, immunoblotting against DGK alpha C-terminus. The soluble fraction after lysis (supernatant) had been stored for two weeks at −80°C (in 20% glycerol); immediately prior to affinity purification, the insoluble fraction was removed by centrifugation at 100,000 × *g* for one hour at 4°C (supernatant's supernatant). (d) Left, elution volumes of molecular weight standards and of purified alphacat from a Sephadex® G-200 column. Left vertical axis, A620 of blue dextran elution and A280 of protein standard elutions. Right vertical axis, quantification of the immunoblot signal from the blot shown at right, mean ± SD (AU). Densitometry of the ~90 kD band was measured three times on the same film using ImageJ. Right, SDS-PAGE followed by immunoblotting against DGK alpha C-terminus. (e) SDS-PAGE of 8% acrylamide gels followed by: top, Coomassie staining; bottom, immunoblotting against DGK alpha C-terminus. U, uninduced; I, induced; L, lysate; S, supernatant (after removing insoluble from lysate). Cam, chloramphenicol.

translation products, and decreased expression of the target protein, even in response to only a single rare codon[75,76]. The cDNA of alphacat does in fact have a number of rare codons: two AGG, five AGA, eight CTA, one ATA, four CGA, twelve CCC, eight GGA, and three CGG. Alphacat TEV in pET32a, when coexpressed with the DnaK/DnaJ/GrpE/ClpB set of chaperones, produces, in addition to the predominant band of the predicted size, an additional, lower band that is recognized by the α-DGK-alpha-C-terminus antibody (Figure 5b, bottom right); alphacat in pET28-HisMBP-FLAGpp (Figure 6b) and alphacat in pT71myc (Figure 1b) likewise produce several recognized bands. These additional bands could indeed be truncations produced by aborted translation or by frameshifting during translation.

Another possible explanation for the greater success for recombinant expression of prokaryotic LCB5 family proteins than of eukaryotic proteins is that eukaryotic proteins expressed in prokaryotic systems may not be properly post-translationally modified. Phosphorylation sites on DGK have been described[24,77,78]: these, or other as-of-yet unannotated post-translational modifications, could be important for protein solubility or stability.

Size may be another factor limiting the success of recombinantly expressing eukaryotic DGKs in prokaryotic systems. *S. typhimurium* YegS and *S. aureus* DgkB are 32 and 35 kD, respectively, smaller than any of the eukaryotic DGKs. Although no absolute upper limit has been reported for the size of proteins that can be recombinantly expressed in *E. coli*, in general, larger proteins express less well. Our own observations are consistent with this rule of thumb: our the smallest construct tested, alphacat in pT71myc, expresses the most robustly, and our alphacat constructs always express at higher levels than their full-length DGK alpha counterparts.

Translational folding partners are frequently used to improve the solubility of proteins expressed in *E. coli*[62–65]. However, our work has demonstrated that adding GST, TRX, or MBP as a fusion tag did not improve the solubility of either full-length DGK or alphacat. All of the constructs in this study are tagged on the N-terminus. The position of a fusion tag can greatly affect a protein's expression and function[79,80]; perhaps exposure of the N-terminus of full-length DGK alpha is required for stability, and a C-terminally tagged construct would express better or be more stable. Alternatively, as discussed above, even the smallest constructs used in this study is large by prokaryotic standards, and perhaps any additional solubility conferred by the fusion tag was counteracted by the fact that the tagged protein was larger in size.

Progress is being made in the ability to predict the ideal fusion tag to solubilize target proteins; however, much work remains to be done. Protein solubility prediction servers[81,82] are invaluable tools, but they sometimes disagree in their predictions. For example, PROSO[82] predicts our full-length DGK alpha in pT71myc construct to be soluble with a probability of 0.520, whereas SOLpro[81] predicts it to be insoluble with a probability of 0.550540. Their predictions may not be always accurate, either: SOLpro[81], for example, predicts the alphacat in pET28-HisMBP-FLAGpp construct to be soluble with a probability of 0.771506, which is contrary to the data we show in Figure 6. Given the difficulty in predicting which solubility tags will work, it is entirely possible that alternative solubility tags could help increase the soluble yield of mammalian DGKs, and perhaps even cause them to elute as a monodisperse population from an analytical gel filtration column. As mentioned above, the NusA tag proved helpful for expressing *A. thaliana* AtDGK2 in *E. coli*[48]; however, this report does not mention whether the purified AtDGK2 was monodisperse. Solubility predictions by SOLpro[81] for NusA-tagged alphacat and full-length DGK alpha are very optimistic, predicting them to be soluble with probabilities of 0.922228 and 0.870324, respectively, whereas predictions by PROSO[82] are more measured: 0.561 and 0.532, respectively, possibly owing to the large size of these constructs (110 and 148 kD, respectively). Tags specifically engineered to improve the solubility of target proteins have been successfully developed in some systems[65], and could be useful for DGK studies; however, at this juncture, improving the solubility of eukaryotic DGKs remains a process of trial-and-error.

Coexpressing alphacat with bacterial chaperones, especially GroEL/ES, increases the yield of some, but not all, of our constructs in the soluble fraction, which is promising for large-scale expressions for crystallography. Unfortunately, alphacat in this soluble fraction still elutes in the void volume during analytical gel filtration chromatography. One reason that alphacat coexpressed with GroEL/ES elutes in the void volume could be explained by its being complexed to the GroEL, based on our evidence that the two proteins copurify on Ni-NTA, and they coelute from the analytical gel filtration column. If the alphacat is in fact complexed with GroEL/ES, the predicted molecular weight of the complex would be greater than 900 kD, and thus would indeed be predicted to elute in the void on the Sephadex® G-200 column. Another possibility is that while coexpressing alphacat with bacterial chaperones is sufficient to increase its yield in the supernatant, it still remains in microscopic aggregates.

The maximum size of a protein to fit in the *cis*-cavity of GroEL has been reported to be 57 kD[83]; on the other hand, GroEL has also been reported to help fold substrates as large as 150 kD[84]. Therefore, it is not entirely surprising that the GroEL/ES sets of chaperones did not improve the solubility of any of the full-length DGK alpha constructs, or of the alphacat in pET32a constructs, although coexpression with GroEL/ES clearly improved the yield of alphacat in pGEX-4T2 in the supernatant after centrifugation, even though the size of the GST-tagged alphacat construct is 71.6 kD.

Analysis of the chaperone data is further complicated by the fact that GroEL is recognized by the α-DGK-alpha antibody (Figure 2b). Endogenous GroEL could thus be the identity of the predominant 60 kD immunoreactive band seen in the partially purified alphacat in pET28-HisMBP-FLAGpp, in which case, GroEL's failing to release alphacat could once again explain why alphacat in pET28-HisMBP-FLAGpp elutes in the void volume from the analytical gel filtration column, even though GroEL was not overexpressed in this preparation.

It is not surprising that the DnaK/DnaJ/GrpE and DnaK/DnaJ/GrpE/ClpB sets of chaperones did not improve the solubility of either alphacat or full-length DGK alpha in any of the constructs tested, seeing as only DnaK appears to overexpress (Figures 2a, 3b, 5b) and its cochaperones DnaJ (which stimulates DnaK's ATPase activity[85]) and GrpE (which acts as a nucleotide exchange factor for DnaK[85]) are not expressed proportionately. DnaK has also been reported to induce proteolysis in response to overproduction of a recombinant protein[86], which may be the reason we observe new, smaller, immunoreactive bands in alphacat TEV in pET32a lysates when coexpressed with the DnaK set of chaperones (Figure 5b, bottom right).

It is entirely possible that coexpression with alternative sets of chaperones could also enhance the solubility of these proteins, but the process of choosing a set of chaperones to coexpress with a given protein remains largely empirical. Other proteins reported to have chaperone activity, and thus potential candidates for coexpression to improve the solubility of eukaryotic DGKs, include Hsp90[87], α-crystallins[88], and dehydrins[89]. DnaK itself indeed would also be a candidate for consideration, as long as its cochaperones DnaJ and GrpE are also appropriately expressed, and could even be coexpressed with GroEL/ES, given that these chaperones can work in parallel[90], thereby delivering the driving force needed to solubilize DGK alpha.

Detergents have often been reported to improve the solubility of recalcitrant proteins[91–93]. Our method for determining monodispersity, analytical gel filtration using a Sephadex® G-200 resin, however, is incompatible with Triton X-100 concentrations as low as 0.01% (v/v) because the detergent causes an unacceptable loss of resolution

in the molecular weight standards (unpublished observations, EP). Future studies wishing to monitor the monodispersity of eukaryotic DGKs may wish to consider alternative resin/detergent combinations.

This body of work aims to provide valuable insight for those wishing to express and purify eukaryotic DGK. By taking into account all the aforementioned considerations, understanding a complex protein like DGK alpha could open up doors for the purification and subsequent structural studies of other challenging proteins and protein/lipid structures.

Methods

Cloning. The pT71myc plasmid was provided by Professor Daniel Leahy's laboratory (Biophysics and Biophysical Chemistry, The Johns Hopkins University School of Medicine); the pET32a plasmid was provided by Professor Cynthia Wolberger's laboratory (Biophysics and Biophysical Chemistry, The Johns Hopkins University School of Medicine); and the pET28-HisMBP-FLAGpp plasmid was provided by Professor Sean Taverna's laboratory (Pharmacology and Molecular Sciences, The Johns Hopkins University School of Medicine). pT71myc is a derivative of the pET28(a) vector; it uses the T7 promoter and contains the kanamycin resistance gene.

SalI and NotI sites, as well as desired protease sites, were added to the full-length DGK alpha or alphacat inserts by the polymerase chain reaction (PCR). These SalI and NotI sites were then used to clone the insert into the plasmid of interest. Successful insertion was confirmed by DNA sequencing.

The chaperone-containing plasmids were provided by Professor Philip Cole's laboratory (Pharmacology and Molecular Sciences, The Johns Hopkins University School of Medicine). The identity, insertion of the chaperones into the provided plasmids, and sequence of the shorter chaperones (GroES and GrpE) were verified by DNA sequencing (The Synthesis & Sequencing Facility, The Johns Hopkins University School of Medicine). A protein-protein BLAST search[94] identified GroEL to be from either *Plesiomonas shigelloides* (GenBank: BAE95977.1) or *E. coli* (NCBI Reference Sequence: YP_006093740.1) with at least two nonsynonymous point mutations. GroES, TF, DnaK, GrpE, and ClpB were likewise identified to be from *E. coli* (NCBI Reference Sequences NP_290775.1, NP_286178.1, NP_285706.1, NP_417104.1, and NP_289147.1, respectively), and DnaJ to be from either *E. coli* (NCBI Reference Sequence: NP_414556.1) or from *Shigella flexneri* (NCBI Reference Sequence: NP_835756.1). Each chaperone plasmid included a chloramphenicol resistance gene, a T7 promoter, and the *lac* operator (LacO). In a single set, all the chaperones are encoded in the plasmid in series (but each with their own stop codon) behind a single promoter, with the exception of GroEL/ES/TF, in which case TF follows a second copy of T7/LacO.

Protein expression. The BL21(DE3) or Rosetta™(DE3) (Novagen®) strains of *E. coli* were transformed with the plasmid(s) of interest, and successful transformants were selected on Luria Bertani (LB) agar (1.5% (w/v)) with the appropriate antibiotic (kanamycin (30 μg/mL) for pT71myc and pET28-HisMBP-FLAGpp, chloramphenicol (35 μg/mL) for the chaperones, and carbenicillin (100 μg/mL) for pGEX-4T2 and pET32a). Either a single colony from a freshly grown LB agar plate, or else a glycerol stock made from such a colony and then stored at −80°C, was used to inoculate LB medium containing the appropriate antibiotic, and the culture was shaken at 225 rotations per minute (rpm) overnight at 37°C. The following morning, a larger culture was inoculated with the starter culture, and shaken at 37°C until the OD600 reached 0.3–1, at which point IPTG was added to 0.1–1 mM to induce expression of the plasmid. IPTG was omitted for uninduced controls. The cultures were then shaken either at 37°C for three hours, or at 16°C overnight (12–22 hours).

The following morning, cells were pelleted by centrifugation (15 minutes at ~5000–20,000 × *g* at 4°C). Cell pellets were resuspended in 4 mL lysis buffer per gram cell pellet, except for full-length alpha and alphacat in pET32a, which were each resuspended in 40 mL lysis buffer per gram cell pellet, and for full-length alpha in pT71myc, which was resuspended in 0.25 mL lysis buffer per mL culture. For full-length alpha and alphacat in pT71myc plus chaperones, in pET32a, and in pET28-HisMBP-FLAPpp, this lysis buffer was 50 mM tris(hydroxymethyl)aminomethane (Tris), pH 8.0, 300 mM NaCl, 10 mM imidazole, 5 mM $MgCl_2$, 1 mM $CaCl_2$, 0.25% (v/v) Triton X-100, 1× protease inhibitor cocktail (Roche 11873580001), 0.5 mM dithiothreitol (DTT); for alphacat in pT71myc without chaperones, this lysis buffer was the same as above except that it was buffered to pH 6.4 with 50 mM 4-(2-hydroxyethyl)-1-piperazineethanesulfonic acid (HEPES), and 0.5% (v/v) Nonidet P-40 (NP-40) was used instead of Triton X-100; and for alphacat in pGEX-4T2, this lysis buffer was 50 mM Tris, pH 8.0, 1 mM $CaCl_2$, 0.25% (v/v) Triton X-100, 1× protease inhibitor cocktail, 5 mM DTT. When time allowed, the resuspended cell pellet was frozen at −80°C, and then rethawed to ensure complete lysis. Egg white lysozyme was added to 1 mg per mL. The resuspended cell pellet was incubated on ice for thirty minutes, vortexing occasionally to mix. The resuspended cell pellet was then lysed by probe sonication in at least ten ten-second bursts, resting on ice between each burst, until no longer viscous. The insoluble fraction was removed by centrifuging at 40,000–120,000 × *g* for 65–90 minutes at 4°C.

Arresting protein translation. After expressing overnight at 20°C, *E. coli* cells were pelleted by centrifugation. The samples annotated as "with Cam" in Figure 6e, both uninduced and induced, were resuspended with LB plus kanamycin plus chloramphenicol (200 μg/mL). Because our chloramphenicol stock solutions are stored as 35 μg/mL in ethanol, "uninduced without Cam" samples were resuspended in LB plus kanamycin plus ethanol (0.6% (v/v)) in order to control for the addition of ethanol along with the chloramphenicol. "Induced without Cam" samples were resuspended in LB plus kanamycin plus IPTG (0.1 mM). The cultures were shaken for another two hours at 20°C, after which cell lysates were harvested as previously described.

Refolding from inclusion bodies. The alphacat in pT1myc lysate was centrifuged at ~100,000 × *g* for 45 minutes at 4°C. The pellet was resuspended in 2.5 mL per gram cell pellet extraction buffer (50 mM HEPES, pH 6.4, 300 mM NaCl, 10 mM imidazole, 5 mM $MgCl_2$, 1 mM $CaCl_2$, 6.8 M guanidinium chloride). To solubilize alphacat from inclusion bodies, the resuspended pellet was probe-sonicated in ten-second bursts, resting on ice between each burst, until clear. The insoluble fraction was removed by centrifuging at ~100,000 × *g* for 30 minutes at 4°C. The protein was refolded by diluting 1 : 50 (v/v) into loading buffer (50 mM HEPES, pH 6.4, 300 mM NaCl, 10 mM imidazole, 5 mM $MgCl_2$, 1 mM $CaCl_2$, 0.5 mM DTT). The insoluble fraction was removed by centrifuging ~20,000 × *g* for 30 minutes at 4°C.

Batch purification: Ni-NTA. Alphacat in pT71myc and in pET28-HisMBP-FLAGpp's fusion tags included hexahistidine, which was used to purify the protein by affinity chromatography to Ni-NTA agarose (QIAGEN® 30210, which is a 50% slurry). After removing the insoluble fraction from either the lysate or the refolded protein, Ni-NTA agarose was directly added 1 : 11-8000 (v/v), and incubated with the protein (2 hours–3 days), rocking at 4°C. The resin was pelleted by centrifugation, and the supernatant was collected as flowthrough. The resin was then washed, and after each wash step, the resin was likewise collected by centrifugation. Purified protein (eluate) was collected from the supernatant after incubating the resin with elution buffer. For alphacat in pT71myc, the wash buffer was 50 mM HEPES, pH 6.4, 300 mM NaCl, 70 mM imidazole, 5 mM $MgCl_2$, 1 mM $CaCl_2$, 0.1 mM tris(2-carboxyethyl)phosphine (TCEP), and the elution buffer was the same except that the imidazole was increased to 250 mM. For alphacat in pT71myc plus chaperones, wash buffer 1 was 50 mM Tris, pH 8.0, 300 mM NaCl, 10 mM imidazole, 1 mM $CaCl_2$, 0.5 mM DTT; wash buffer 2 was the same except that it was buffered to pH 6.4 with 55 mM sodium citrate and also included 5 mM $MgCl_2$; wash buffer 3 was the same as wash buffer 2 except that imidazole was increased to 70 mM; elution buffer 1 had 250 mM imidazole; and elution buffer 2 had 500 mM imidazole. For alphacat in pET28-HisMBP-FLAGpp, wash buffer 1 was the same as for alphacat in pT71myc plus chaperones; wash buffer 2 was the same except that the imidazole was increased to 70 mM; elution buffer 1 had 250 mM imidazole; and elution buffer 2 had 500 mM imidazole.

Batch purification: Magne-GST™. Alphacat in pGEX-4T2's fusion tags included GST, which was used to purify the protein by affinity chromatography to Magne-GST™ glutathione particles (Promega V8611). Magne-GST™ beads were prewashed in wash buffer (50 mM Tris, pH 8.0, 140 mM NaCl, 10 mM KCl, 1 mM $CaCl_2$, 0.25% (v/v) Triton X-100, 1× protease inhibitor cocktail, 5 mM DTT). 46.9 μL washed beads per gram cell pellet were added to the lysate after the insoluble fraction had been removed, and rocked at 4°C for 75 minutes. The beads were pelleted by magnet, and the supernatant was collected as flowthrough. The beads were washed with wash buffer and then eluted with elution buffer 1 (the same as wash buffer, except with 0.1 mM glutathione), elution buffer 2 (0.3 mM glutathione), elution buffer 3 (0.5 mM glutathione), elution buffer 4 (1.5 mM glutathione), and elution buffer 5 (100 mM glutathione).

Analytical gel filtration. The analytical gel filtration resin used was Sephadex® G-200 (Sigma G-200-120). All analytical gel filtration steps were carried out at 4°C. The resin was hydrated in and equilibrated by gravity with gel filtration buffer. For alphacat in pT71myc, the gel filtration buffer was 55 mM HEPES, 250 mM imidazole, 5 mM $MgCl_2$, 1 mM $CaCl_2$, pH 6.4; for alphacat in pT71myc plus chaperones the gel filtration buffer was the same except that it was buffered to pH 6.4 with 55 mM sodium citrate; for alphacat in pGEX-4T2 plus chaperones the gel filtration buffer was 50 mM Tris, 100 mM KCl, pH 8.0; and for alphacat in pET28-HisMBP-FLAGpp the gel filtration buffer was 50 mM Tris, 300 mM NaCl, 250 mM imidazole, 5 mM $MgCl_2$, 1 mM $CaCl_2$, pH 8.0. The column was calibrated in each buffer system by gravity flow with blue dextran (~2000 kD), sweet potato β-amylase (200 kD), yeast alcohol dehydrogenase (150 kD), bovine serum albumin (66 kD), and/or bovine erythrocyte carbonic anhydrase (29 kD). The void volume (V_o) was measured by summing the volumes of the fractions up to and including the fraction with the maximum absorbance at 620 nm. The elution volume (V_e) for each protein standard was measured by summing the volumes of the fractions up to and including the fraction with the maximum absorbance at 280 nm.

Before loading alphacat, the column was blocked with albumin (10 mg/mL, 1/20th of the column bed volume), and then washed with two to three times the V_e of albumin with gel filtration buffer. When necessary, prior to loading purified alphacat was concentrated by dialyzing against dialysis buffer (gel filtration buffer plus 15% (w/v) polyethylene glycol (PEG) 17.5 kD) using either a 10,000 molecular weight cut-off (MWCO) cassette or 3.5 kD MWCO dialysis tubing. Immediately before loading, the insoluble fraction of purified alphacat was removed by centrifuging at 40,000 × *g* for 90 minutes at 4°C. The soluble fraction was then loaded onto the gel filtration resin (at a volume no greater than 1/20th the column bed volume). Fractions were collected,

and the volume of each fraction was measured. In the case of alphacat in pT71myc, the protein concentration of each fraction was measured by the Bio-Rad Protein Assay (500-0006). In the case of alphacat in pT71myc plus chaperones, alphacat in pGEX-4T2, and alphacat in PET28-HisMBP-FLAGpp, the fractions were analyzed by immunoblotting to determine the elution volume.

SDS-PAGE. Because SDS precipitates with guanidine and with potassium, guanidine and/or potassium was removed from guanidine or potassium-containing samples by ethanol-precipitation and washing the protein pellet before combining with SDS gel-loading-buffer.

Standard laboratory methods were used for protein electrophoresis. For immunoblotting, the primary antibodies used were, for Figure 1b, mouse α-His (Abcam ab6196[95] (1 : 2500 (v/v))), for Figure 3, mouse α-His_6 (Clontech 631212[96] (1 : 5000 (v/v))), and for the other figures, rabbit α-DGK-alpha-C-term (Abgent AP8128b[31] (1 : 300 (v/v))).

Exposures faint enough that text could be read through the bands of interest were selected for densitometry. Densitometry was measured by ImageJ (see "Equipment and Settings").

Equipment and settings. The Odyssey® Infrared Imaging System running Odyssey® v3.0 (LI-COR®) was used to scan the immunoblots shown in Figure 3. The membranes were scanned with a resolution of 169 μm, quality of medium, offset of 0.0, and intensity of 5. The 700 channel is shown.

Film that had been exposed to immunoblots was scanned as 1200 dots per inch (dpi) .tiff files. Densitometry of these files was measured by ImageJ[97] (v1.46r) without calibration, three times from the same film. The relative densitometry of each lane was normalized to the total densitometry of all the lanes on that replicate. The means and standard deviations (SigmaPlot 12) of three normalized densitometries for each lane are displayed in the figures shown here.

1. Takeishi, Y., Goto, K. & Kubota, I. Role of diacylglycerol kinase in cellular regulatory processes: a new regulator for cardiomyocyte hypertrophy. *Pharmacol. Ther.* **115**, 352–359 (2007).
2. Ali, H. *et al*. Selective translocation of diacylglycerol kinase zeta in hippocampal neurons under transient forebrain ischemia. *Neurosci. Lett.* **372**, 190–195 (2004).
3. Kanoh, H. & Ohno, K. Partial purification and properties of diacylglycerol kinase from rat liver cytosol. *Arch. Biochem. Biophys.* **209**, 266–275 (1981).
4. Besterman, J. M., Pollenz, R. S., Booker, E. L. Jr. & Cuatrecasas, P. Diacylglycerol-induced translocation of diacylglycerol kinase: use of affinity-purified enzyme in a reconstitution system. *Proc. Natl. Acad. Sci. U.S.A.* **83**, 9378–9382 (1986).
5. Stathopoulos, V. M. *et al*. Identification of two cytosolic diacylglycerol kinase isoforms in rat brain, and in NIH-3T3 and ras-transformed fibroblasts. *Biochem. J.* **272**, 569–575 (1990).
6. Chen, Q., Klemm, N. & Jeng, I. Characterization of two cytosolic diacylglycerol kinase forms. *J. Neurochem.* **60**, 1212–1219 (1993).
7. Shim, Y. H., Lin, C. H. & Strickland, K. P. The purification and properties of monoacylglycerol kinase from bovine brain. *Biochem. Cell Biol.* **67**, 233–241 (1989).
8. Ogawara, H. *et al*. Inhibitors of diacylglycerol kinase from Drechslera sacchari. *J. Antibiot.* **47**, 499–501 (1994).
9. Yada, Y., Ozeki, T., Kanoh, H. & Nozawa, Y. Purification and characterization of cytosolic diacylglycerol kinases of human platelets. *J. Biol. Chem.* **265**, 19237–19243 (1990).
10. Hodgkin, M., Gardner, S. & Wakelam, M. The identification of several stearoyl-arachidonyl selective diacylglycerol kinases in the particulate fraction of porcine testes. *Biochem. Soc. Trans.* **21**, 490S (1993).
11. Redman, C., Lefevre, J. & MacDonald, M. L. Inhibition of diacylglycerol kinase by the antitumor agent calphostin C. Evidence for similarity between the active site of diacylglycerol kinase and the regulatory site of protein kinase C. *Biochem. Pharmacol.* **50**, 235–241 (1995).
12. Jiang, Y., Sakane, F., Kanoh, H. & Walsh, J. P. Selectivity of the diacylglycerol kinase inhibitor 3-{2-(4-[bis-(4-fluorophenyl)methylene]-1-piperidinyl)ethyl}-2,3-dihydro -2-thioxo-4(1H)quinazolinone (R59949) among diacylglycerol kinase subtypes. *Biochem. Pharmacol.* **59**, 763–772 (2000).
13. Jiang, Y., Qian, W. J., Hawes, J. W. & Walsh, J. P. A domain with homology to neuronal calcium sensors is required for calcium-dependent activation of diacylglycerol kinase alpha. *J. Biol. Chem.* **275**, 34092–34099 (2000).
14. Lemaitre, R. N., King, W. C., MacDonald, M. L. & Glomset, J. A. Distribution of distinct arachidonoyl-specific and non-specific isoenzymes of diacylglycerol kinase in baboon (Papio cynocephalus) tissues. *Biochem. J.* **266**, 291–299 (1990).
15. Walsh, J. P., Suen, R., Lemaitre, R. N. & Glomset, J. A. Arachidonoyl-diacylglycerol kinase from bovine testis. Purification and properties. *J. Biol. Chem.* **269**, 21155–21164 (1994).
16. Walsh, J. P., Suen, R. & Glomset, J. A. Arachidonoyl-diacylglycerol kinase. Specific in vitro inhibition by polyphosphoinositides suggests a mechanism for regulation of phosphatidylinositol biosynthesis. *J. Biol. Chem.* **270**, 28647–28653 (1995).
17. Thomas, W. E. & Glomset, J. A. Multiple Factors Influence the Binding of a Soluble, Ca2+-Independent, Diacylglycerol Kinase to Unilamellar Phosphoglyceride Vesicles. *Biochemistry* **38**, 3310–3319 (1999).
18. Thomas, W. E. & Glomset, J. A. Affinity purification and catalytic properties of a soluble, Ca2+-independent, diacylglycerol kinase. *Biochemistry* **38**, 3320–3326 (1999).
19. Inoue, H., Yoshioka, T. & Hotta, Y. Partial purification and characterization of membrane-associated diacylglycerol kinase of Drosophila heads. *Biochim. Biophys. Acta* **1122**, 219–224 (1992).
20. Wissing, J. B. & Wagner, K. G. Diacylglycerol kinase from suspension cultured plant cells: characterization and subcellular localization. *Plant Physiol.* **98**, 1148–1153 (1992).
21. Kanoh, H., Kondoh, H. & Ono, T. Diacylglycerol kinase from pig brain. Purification and phospholipid dependencies. *J. Biol. Chem.* **258**, 1767–1774 (1983).
22. Kanoh, H. & Ono, T. Utilization of diacylglycerol in phospholipid bilayers by pig brain diacylglycerol kinase and Rhizopus arrhizus lipase. *J. Biol. Chem.* **259**, 11197–11202 (1984).
23. Bishop, H. H. & Strickland, K. P. Comparisons of monoacylglycerols and diacylglycerols of varying fatty acid composition as substrates for the acylglycerol kinase(s) of rat brain. *Lipids* **15**, 285–291 (1980).
24. Kanoh, H., Yamada, K., Sakane, F. & Imaizumi, T. Phosphorylation of diacylglycerol kinase in vitro by protein kinase C. *Biochem. J.* **258**, 455–462 (1989).
25. Sakane, F., Yamada, K. & Kanoh, H. Different effects of sphingosine, R59022 and anionic amphiphiles on two diacylglycerol kinase isozymes purified from porcine thymus cytosol. *FEBS Letters* **255**, 409–413 (1989).
26. Sakane, F., Yamada, K., Imai, S. & Kanoh, H. Porcine 80-kDa diacylglycerol kinase is a calcium-binding and calcium/phospholipid-dependent enzyme and undergoes calcium-dependent translocation. *J Biol Chem* **266**, 7096–100 (1991).
27. Lin, C. H., Bishop, H. & Strickland, K. P. Properties of diacylglycerol kinase purified from bovine brain. *Lipids* **21**, 206–211 (1986).
28. Kato, M. & Takenawa, T. Purification and characterization of membrane-bound and cytosolic forms of diacylglycerol kinase from rat brain. *J. Biol. Chem.* **265**, 794–800 (1990).
29. Kahn, D. W. & Besterman, J. M. Cytosolic rat brain synapsin I is a diacylglycerol kinase. *Proc. Natl. Acad. Sci. U.S.A.* **88**, 6137–6141 (1991).
30. Younes, A. *et al.* Ceramide is a competitive inhibitor of diacylglycerol kinase in vitro and in intact human leukemia (HL-60) cells. *J. Biol. Chem.* **267**, 842–847 (1992).
31. Schaap, D. *et al.* Purification, cDNA-cloning and expression of human diacylglycerol kinase. *FEBS Lett.* **275**, 151–158 (1990).
32. Haq, E., Sharma, S. & Khuller, G. K. Purification of diacylglycerol kinase from Microsporum gypseum and its phosphorylation by the catalytic subunit of protein kinase A. *Arch. Biochem. Biophys.* **392**, 219–225 (2001).
33. Sakane, F., Yamada, K., Kanoh, H., Yokoyama, C. & Tanabe, T. Porcine diacylglycerol kinase sequence has zinc finger and E-F hand motifs. *Nature* **344**, 345–348 (1990).
34. Katagiri, T., Mizoguchi, T. & Shinozaki, K. Molecular cloning of a cDNA encoding diacylglycerol kinase (DGK) in Arabidopsis thaliana. *Plant Mol. Biol.* **30**, 647–653 (1996).
35. Topham, M. K. & Prescott, S. M. Diacylglycerol Kinase ζ Regulates Ras Activation by a Novel Mechanism. *J Cell Biol* **152**, 1135–1144 (2001).
36. Takahashi, M., Yamamoto, T., Sakai, H. & Sakane, F. Calcium negatively regulates an intramolecular interaction between the N-terminal recoverin homology and EF-hand motif domains and the C-terminal C1 and catalytic domains of diacylglycerol kinase α. *Biochem. Biophys. Res. Commun.* **423**, 571–576 (2012).
37. Sanjuán, M. A., Jones, D. R., Izquierdo, M. & Mérida, I. Role of diacylglycerol kinase alpha in the attenuation of receptor signaling. *J. Cell Biol.* **153**, 207–220 (2001).
38. Imai, S., Kai, M., Yasuda, S., Kanoh, H. & Sakane, F. Identification and characterization of a novel human type II diacylglycerol kinase, DGK kappa. *J. Biol. Chem* **280**, 39870–39881 (2005).
39. Lung, M. *et al.* Diacylglycerol kinase epsilon is selective for both acyl chains of phosphatidic acid or diacylglycerol. *J. Biol. Chem.* **284**, 31062–31073 (2009).
40. Dicu, A. O., Topham, M. K., Ottaway, L. & Epand, R. M. Role of the hydrophobic segment of diacylglycerol kinase epsilon. *Biochemistry* **46**, 6109–6117 (2007).
41. Luo, B., Prescott, S. M. & Topham, M. K. Association of diacylglycerol kinase zeta with protein kinase C alpha: spatial regulation of diacylglycerol signaling. *J. Cell Biol.* **160**, 929–937 (2003).
42. Sakane, F., Kai, M., Wada, I., Imai, S. & Kanoh, H. The C-terminal part of diacylglycerol kinase alpha lacking zinc fingers serves as a catalytic domain. *Biochem. J* **318 (Pt2)**, 583–590 (1996).
43. De la Roche, M. A. *et al.* Dictyostelium discoideum has a single diacylglycerol kinase gene with similarity to mammalian θ isoforms. *Biochemical Journal* **368**, 809 (2002).
44. Ostroski, M., Tu-Sekine, B. & Raben, D. M. Analysis of a Novel Diacylglycerol Kinase from Dictyostelium discoideum: DGKA. *Biochemistry* **44**, 10199–10207 (2005).
45. Ahmed, S. *et al.* The cysteine-rich domain of human proteins, neuronal chimaerin, protein kinase C and diacylglycerol kinase binds zinc. Evidence for the involvement of a zinc-dependent structure in phorbol ester binding. *Biochem J.* **280**, 233–241 (1991).

46. Sakane, F., Imai, S., Yamada, K. & Kanoh, H. The regulatory role of EF-hand motifs of pig 80 K diacylglycerol kinase as assessed using truncation and deletion mutants. *Biochem. Biophys. Res. Commun* **181**, 1015–1021 (1991).
47. Liu, Z., Chang, G. Q. & Leibowitz, S. F. Diacylglycerol kinase zeta in hypothalamus interacts with long form leptin receptor. Relation to dietary fat and body weight regulation. *J. Biol. Chem.* **276**, 5900–5907 (2001).
48. Gómez-Merino, F. C. *et al.* AtDGK2, a novel diacylglycerol kinase from Arabidopsis thaliana, phosphorylates 1-stearoyl-2-arachidonoyl-sn-glycerol and 1,2-dioleoyl-sn-glycerol and exhibits cold-inducible gene expression. *J. Biol. Chem.* **279**, 8230–8241 (2004).
49. Gómez-Merino, F. C. *et al.* Arabidopsis AtDGK7, the smallest member of plant diacylglycerol kinases (DGKs), displays unique biochemical features and saturates at low substrate concentration: the DGK inhibitor R59022 differentially affects AtDGK2 and AtDGK7 activity in vitro and alters plant growth and development. *J. Biol. Chem.* **280**, 34888–34899 (2005).
50. Prodeus, A., Berno, B., Topham, M. K. & Epand, R. M. The basis of the substrate specificity of the epsilon isoform of human diacylglycerol kinase is not a consequence of competing hydrolysis of ATP. *Chem. Phys. Lipids* **166C**, 26–30 (2012).
51. Tu-Sekine, B. & Raben, D. M. Dual regulation of diacylglycerol kinase (DGK)-θ: polybasic proteins promote activation by phospholipids and increase substrate affinity. *J. Biol. Chem.* **287**, 41619–41627 (2012).
52. Yamada, K., Sakane, F., Matsushima, N. & Kanoh, H. EF-hand motifs of alpha, beta and gamma isoforms of diacylglycerol kinase bind calcium with different affinities and conformational changes. *Biochem. J* **321 (Pt1)**, 59–64 (1997).
53. Liu, G., Shao, Y., Xiao, R., Acton, T., Montelione, G. T. & Szyperski, T. Northeast Structural Genomics Consortium. NMR structure of the diacylglycerol kinase alpha, NESGC target HR532. PDB ID: 1TUZ.
54. Miyamoto, K., Tomizawa, T., Koshiba, S., Inoue, M., Kigawa, T. & Yokoyama, S. Solution structure of the C1 domain of the human diacylglyerol kinase delta. PDB ID: 1R79.
55. Harada, B. T. *et al.* Regulation of enzyme localization by polymerization: polymer formation by the SAM domain of diacylglycerol kinase delta1. *Structure* **16**, 380–387 (2008).
56. Marchler-Bauer, A. *et al.* CDD: conserved domains and protein three-dimensional structure. *Nucleic Acids Res.* **41**, D348–352 (2013).
57. Palmer, I. & Wingfield, P. T. Preparation and extraction of insoluble (inclusion-body) proteins from *Escherichia coli*. *Current Protocols in Protein Science* 6.3.1–6.3.18 (2004).
58. Thomas, J. G., Ayling, A. & Baneyx, F. Molecular chaperones, folding catalysts, and the recovery of active recombinant proteins from E. coli. To fold or to refold. *Appl. Biochem. Biotechnol* **66**, 197–238 (1997).
59. De Marco, A. Protocol for preparing proteins with improved solubility by co-expressing with molecular chaperones in Escherichia coli. *Nat Protoc* **2**, 2632–2639 (2007).
60. Haacke, A., Fendrich, G., Ramage, P. & Geiser, M. Chaperone over-expression in Escherichia coli: apparent increased yields of soluble recombinant protein kinases are due mainly to soluble aggregates. *Protein Expr. Purif* **64**, 185–193 (2009).
61. Kipnis, Y., Papo, N., Haran, G. & Horovitz, A. Concerted ATP-induced allosteric transitions in GroEL facilitate release of protein substrate domains in an all-or-none manner. *Proceedings of the National Academy of Sciences* **104**, 3119–3124 (2007).
62. Dyson, M. R., Shadbolt, S. P., Vincent, K. J., Perera, R. L. & McCafferty, J. Production of soluble mammalian proteins in Escherichia coli: identification of protein features that correlate with successful expression. *BMC Biotechnol.* **4**, 32 (2004).
63. Douette, P. *et al.* Escherichia coli fusion carrier proteins act as solubilizing agents for recombinant uncoupling protein 1 through interactions with GroEL. *Biochem. Biophys. Res. Commun.* **333**, 686–693 (2005).
64. Esposito, D. & Chatterjee, D. K. Enhancement of soluble protein expression through the use of fusion tags. *Curr. Opin. Biotechnol* **17**, 353–358 (2006).
65. Santner, A. A. *et al.* Sweeping Away Protein Aggregation with Entropic Bristles: Intrinsically Disordered Protein Fusions Enhance Soluble Expression. *Biochemistry* **51**, 7250–7262 (2012).
66. Smith, D. B. Generating fusions to glutathione S-transferase for protein studies. *Meth. Enzymol.* **326**, 254–270 (2000).
67. Smith, D. B. & Johnson, K. S. Single-step purification of polypeptides expressed in Escherichia coli as fusions with glutathione S-transferase. *Gene* **67**, 31–40 (1988).
68. LaVallie, E. R. *et al.* A thioredoxin gene fusion expression system that circumvents inclusion body formation in the E. coli cytoplasm. *Biotechnology (N.Y.)* **11**, 187–193 (1993).
69. Richarme, G. & Caldas, T. D. Chaperone properties of the bacterial periplasmic substrate-binding proteins. *J. Biol. Chem.* **272**, 15607–15612 (1997).
70. Sachdev, D. & Chirgwin, J. M. Fusions to maltose-binding protein: control of folding and solubility in protein purification. *Meth. Enzymol.* **326**, 312–321 (2000).
71. De Marco, A., Deuerling, E., Mogk, A., Tomoyasu, T. & Bukau, B. Chaperone-based procedure to increase yields of soluble recombinant proteins produced in E. coli. *BMC Biotechnol* **7**, 32–32 (2007).
72. Nichols, C. E. *et al.* Characterization of Salmonella typhimurium YegS, a putative lipid kinase homologous to eukaryotic sphingosine and diacylglycerol kinases. *Proteins: Structure, Function, and Bioinformatics* **68**, 13–25 (2007).
73. Bakali, H. M. A., Nordlund, P. & Hallberg, B. M. Expression, purification, crystallization and preliminary diffraction studies of the mammalian DAG kinase homologue YegS from Escherichia coli. *Acta Crystallogr Sect F Struct Biol Cryst Commun* **62**, 295–297 (2006).
74. Miller, D. J., Jerga, A., Rock, C. O. & White, S. W. Analysis of the Staphylococcus aureus DgkB Structure Reveals a Common Catalytic Mechanism for the Soluble Diacylglycerol Kinases. *Structure* **16**, 1036–1046 (2008).
75. Kane, J. F. Effects of rare codon clusters on high-level expression of heterologous proteins in Escherichia coli. *Curr. Opin. Biotechnol.* **6**, 494–500 (1995).
76. Carstens, C.-P. In *E. coli Gene Expression Protocols* **205**, 225–234 (Humana Press).
77. Kanoh, H. & Ono, T. Phosphorylation of pig brain diacylglycerol kinase by endogenous protein kinase. *FEBS Lett.* **201**, 97–100 (1986).
78. Schaap, D., Van der Wal, J., Van Blitterswijk, W. J., Van der Bend, R. L. & Ploegh, H. L. Diacylglycerol kinase is phosphorylated in vivo upon stimulation of the epidermal growth factor receptor and serine/threonine kinases, including protein kinase C-epsilon. *Biochem. J.* **289 (Pt3)**, 875–881 (1993).
79. Palmer, E. & Freeman, T. Investigation Into the use of C- and N-terminal GFP Fusion Proteins for Subcellular Localization Studies Using Reverse Transfection Microarrays. *Comp Funct Genomics* **5**, 342–353 (2004).
80. Gan, X. & Gould, S. J. Identification of an inhibitory budding signal that blocks the release of HIV particles and exosome/microvesicle proteins. *Mol. Biol. Cell* **22**, 817–830 (2011).
81. Magnan, C. N., Randall, A. & Baldi, P. SOLpro: accurate sequence-based prediction of protein solubility. *Bioinformatics* **25**, 2200–2207 (2009).
82. Smialowski, P. *et al.* Protein solubility: sequence based prediction and experimental verification. *Bioinformatics* **23**, 2536–2542 (2007).
83. Sakikawa, C., Taguchi, H., Makino, Y. & Yoshida, M. On the Maximum Size of Proteins to Stay and Fold in the Cavity of GroEL underneath GroES. *J. Biol. Chem.* **274**, 21251–21256 (1999).
84. Houry, W. A., Frishman, D., Eckerskorn, C., Lottspeich, F. & Hartl, F. U. Identification of in vivo substrates of the chaperonin GroEL. *Nature* **402**, 147–154 (1999).
85. Liberek, K., Marszalek, J., Ang, D., Georgopoulos, C. & Zylicz, M. Escherichia coli DnaJ and GrpE heat shock proteins jointly stimulate ATPase activity of DnaK. *Proc. Natl. Acad. Sci. U.S.A.* **88**, 2874–2878 (1991).
86. Martínez-Alonso, M., García-Fruitós, E., Ferrer-Miralles, N., Rinas, U. & Villaverde, A. Side effects of chaperone gene co-expression in recombinant protein production. *Microb Cell Fact* **9**, 64 (2010).
87. Wiech, H., Buchner, J., Zimmermann, R. & Jakob, U. Hsp90 chaperones protein folding in vitro. *Nature* **358**, 169–170 (1992).
88. Narberhaus, F. Alpha-crystallin-type heat shock proteins: socializing minichaperones in the context of a multichaperone network. *Microbiol. Mol. Biol. Rev.* **66**, 64–93; table of contents (2002).
89. Close, T. J. Dehydrins: A commonalty in the response of plants to dehydration and low temperature. *Physiologia Plantarum* **100**, 291–296 (1997).
90. Buchberger, A., Schröder, H., Hesterkamp, T., Schönfeld, H.-J. & Bukau, B. Substrate Shuttling Between the DnaK and GroEL Systems Indicates a Chaperone Network Promoting Protein Folding. *Journal of Molecular Biology* **261**, 328–333 (1996).
91. Long, F., Cho, W. & Ishii, Y. Expression and purification of 15N- and 13C-isotope labeled 40-residue human Alzheimer's β-amyloid peptide for NMR-based structural analysis. *Protein Expr. Purif.* **79**, 16–24 (2011).
92. Park, D.-W. *et al.* Improved recovery of active GST-fusion proteins from insoluble aggregates: solubilization and purification conditions using PKM2 and HtrA2 as model proteins. *BMB Rep* **44**, 279–284 (2011).
93. Black, M. M., Stockum, C., Dickson, J. M., Putterill, J. & Arcus, V. L. Expression, purification and characterisation of GIGANTEA: A circadian clock-controlled regulator of photoperiodic flowering in plants. *Protein Expression and Purification* **76**, 197–204 (2011).
94. Altschul, S. F. *et al.* Gapped BLAST and PSI-BLAST: a new generation of protein database search programs. *Nucleic Acids Res.* **25**, 3389–3402 (1997).
95. Allison, R. *et al.* Two distinct Staufen isoforms in Xenopus are vegetally localized during oogenesis. *RNA* **10**, 1751–1763 (2004).
96. Pollice, A. *et al.* TBP-1 protects the human oncosuppressor p14ARF from proteasomal degradation. *Oncogene* **26**, 5154–5162 (2007).
97. Schneider, C. A., Rasband, W. S. & Eliceiri, K. W. NIH Image to ImageJ: 25 years of image analysis. *Nat. Methods* **9**, 671–675 (2012).

Acknowledgments

We would like to thank all members of the Raben laboratory, as well as Professors Daniel Leahy, Mario Amzel, and Sandra Gabelli (Biophysics and Biophysical Chemistry, The Johns Hopkins University School of Medicine) for helpful discussions; Dr. Bryan Geisbrecht of Professor Daniel Leahy's laboratory for providing the pT71myc plasmid; Dr. Rishi Porecha for cloning alphacat into pT71myc; Ms. Michele Ostroski for cloning alphacat into pGEX-4T2; Mr. David Bolduc of Professor Philip Cole's laboratory (Pharmacology and Molecular Sciences, The Johns Hopkins University School of Medicine) for providing the chaperone plasmids; Dr. Becky Tu-Sekine for transforming the chaperone plasmids into BL21(DE3); Dr. Nadine Samara of Professor Cynthia Wolberger's laboratory (Biophysics and Biophysical Chemistry, The Johns Hopkins University School of Medicine) for providing the pET32a plasmid; Ms. Tonya Gilbert of Professor Sean Taverna's laboratory

(Pharmacology and Molecular Sciences, The Johns Hopkins University School of Medicine) for providing the pET28-HisMBP-FLAGpp plasmid; Dr. Agedi Boto of Professor Mario Amzel's laboratory for support scaling up the expression of alphacat in pT71myc in *E. coli*; Ms. Hana Goldschmidt for performing the protein electrophoresis shown in Figure 2b; Professor Albert Mildvan (Biological Chemistry, The Johns Hopkins University School of Medicine) for providing the Sephadex® G-200 resin; the laboratory of Professor Gerald Hart (Biological Chemistry, The Johns Hopkins University School of Medicine) for the use of their shaking incubator, centrifuges, probe sonicator, and spectrophotometer; the laboratory of Professor Jun Liu (Pharmacology and Molecular Sciences, The Johns Hopkins University School of Medicine) for the use of their spectrophotometer; the laboratory of Professor Jeffry Corden (Molecular Biology & Genetics, The Johns Hopkins University School of Medicine) for the use of their Odyssey® Infrared Imaging System; the Department of Cell Biology (The Johns Hopkins University School of Medicine) for the use of the ultracentrifuge; the Department of Biological Chemistry (The Johns Hopkins University School of Medicine) for the use of the film developer; and Dr. Sabina Muend for help editing the manuscript. This work was supported by an American Heart Association Predoctoral Fellowship (to EP) and by Grant GM059251 from the National Institutes of Health (to DMR).

Author contributions

E.P. designed and performed the experiments (with the exception of what is specifically mentioned in the Acknowledgments section) with guidance from D.M.R. E.P. wrote and D.M.R. reviewed the manuscript.

Additional information

Competing financial interests: The authors declare no competing financial interests.

How to cite this article: Petro, E.J. & Raben, D.M. Bacterial expression strategies for several *Sus scrofa* diacylglycerol kinase alpha constructs: solubility challenges. *Sci. Rep.* **3**, 1609; DOI:10.1038/srep01609 (2013).